Synthesis and Luminescence Properties of Colloidal YVO_4:Eu Phosphors

Arnaud Huignard, Thierry Gacoin, and Jean-Pierre Boilot*

Groupe de Chimie du Solide, Laboratoire de Physique de la Matière Condensée, UMR CNRS 7643, Ecole Polytechnique, 91128 Palaiseau, France

Received November 10, 1999. Revised Manuscript Received January 31, 2000

Concentrated colloidal solutions of well-dispersed YVO_4:Eu nanoparticles are synthesized by precipitation reactions at room temperature and stabilized by sodium hexametaphosphate. X-ray diffraction and electron microscopy characterizations show that the crystalline nanoparticles exhibit an ellipsoidal form with two characteristic dimensions of around 15 and 30 nm. In comparison with the bulk, a lower luminescence efficiency as well as a higher concentration quenching are observed. These deviations are explained as the variations of some characteristics of the colloidal samples, such as the crystallinity and the surface chemistry. When these parameters are optimized, the quantum yield of the luminescence reaches 38% for the nanoparticles containing a europium concentration of 15%.

Introduction

Inorganic luminescent materials have practical applications in almost any device involving the artificial production of light. Cathode ray tubes, lamps, and X-ray detectors are well-known examples.[1] More recently, the development of flat electroluminescent, plasma, or field emission displays with huge industrial applications has increased the demand for materials with increasingly better characteristics in term of stability, brightness, and industrial processing ability.[2]

Recent orientations for the development of new materials concern the research of new chemical compositions less than the optimization of the extrinsic properties of usual phosphors. Grain size, morphology, agglomeration, or surface passivation are indeed well-known to have an impact on the phosphor efficiency.[3] However, the synthesis of conventional phosphor powders involves high-temperature solid-state reactions which provide agglomerated powders with a grain size in the 5−20 μm range. Such conditions do not allow one to easily change the structural characteristics of the obtained powders.

Now, the development of new methods for the production of micron or submicron powders may increase the possibilities for better control of the structural parameters. Among these techniques, colloid chemistry has proved to be very powerful in the synthesis of nonagglomerated nanoparticles with surface accessibility for passivation treatments and the ability to be used in thin-film techniques related to the sol−gel process. A good example is provided by the intensive research on chalcogenide materials which has led to the synthesis of core/shell nanostructures (CdSe/ZnS[4]) or doped nanoparticles (ZnS:Mn[5] and CdS:Mn[6]) with very narrow size distributions and high luminescence quantum yields.

The basic idea of this work is to explore the potentialities of the colloid chemistry for the synthesis of doped oxide phosphors in the nanometer size range. Only very few studies[7] have been reported on this subject yet, probably because of the small number of compounds which can be synthesized under conditions compatible with the colloid chemistry. Yttrium orthovanadate (YVO_4) is a good candidate for such studies, since the bulk material exhibits a high luminescence efficiency[8,9] and since it can be obtained in its crystallized form by precipitation reactions at low temperatures. In a recent paper, Riwotzki and Haase[10] reported on an hydrothermal synthesis at 200 °C of YVO_4:Eu powders, which can be weakly dispersed as an aqueous colloid. The measurement of the luminescence quantum yield was found to be 15% at room temperature.

In this paper, we describe an optimized synthesis of colloidal YVO_4:Eu nanoparticles through classical precipitation reactions. This leads to concentrated and highly luminescent aqueous colloids which are stable in a large pH range. Besides, by keeping the size of the particles around 30 nm, the chosen process allows for the variation of some other important characteristics such as the crystallinity, the defect concentration, and the lattice distortions around the Eu^{3+} sites. Strong correlations with the luminescence behavior of the particles enable us to discriminate the parameters

(1) Blasse, G.; Grabmeier, B. C. *Luminescent Materials*; Springer-Verlag: Berlin, 1994.
(2) Ballato, J.; Lewis, J. S., III; Holloway, P. *MRS Bull.* **1999**, *24* (9), 51.
(3) Bredol, M.; Kynast, U.; Ronda, C. *Adv. Mater.* **1991**, *7/8*, 361.
(4) Kortan, A. R.; Hull, R.; Opila, R. L.; Bawendi, M. G.; Steigerwald, M. L.; Carrol, P. J.; Brus, L. E. *J. Am. Chem. Soc.* **1990**, *112*, 1327. Hines, M. A.; Guyot-Genest, P. *J. Phys. Chem.* **1996**, *100*, 468. Peng, X.; Schlamp, M. C.; Kadavanich, A. V.; Alivisatos, A. P. *J. Am. Chem. Soc.* **1997**, *119*, 7019.
(5) Bhargava, R. N.; Gallagher, D.; Hong, X.; Nurmikko, A. *Phys. Rev. Lett.* **1994**, *72*, 416.
(6) Counio, G.; Esnouf, S.; Gacoin, T.; Boilot, J.-P. *J. Phys. Chem. B* **1996**, *100*, 20021. Counio, G.; Gacoin, T.; Boilot, J.-P. *J. Phys. Chem. B* **1998**, *102*, 5257.
(7) Schmidt, T.; Müller, G.; Spanhel, L.; Kerkel, K.; Forchel, A. *Chem. Mater.* **1998**, *10*, 65.
(8) Levine, A. K.; Palilla, F. C. *Appl. Phys. Lett.* **1964,** *5* (6), 118.
(9) Ropp, R. C. *Luminescence and the Solid State*; Elsevier: Amsterdam, 1991.
(10) Riwotzki, K.; Haase, M. *J. Phys. Chem. B* **1998**, *102*, 10129−10135.

10.1021/cm990722t CCC: $19.00
Published on Web 03/29/2000

responsible for the limited efficiency of the nanoparticles compared to the bulk material.

Experimental Section

The synthesis of yttrium orthovanadate by aqueous precipitation reactions was first reported in 1965 in the work of Arbit and Serebrennikov.[11] Since then, many authors have studied this synthesis, starting from different precursors and varying experimental conditions.[12,13] Among them, Ropp and Carroll[14] studied the titration of Y^{3+} and VO^{2+} acidic solutions by NaOH. They showed that the complete formation of yttrium orthovanadate occurs only when the pH of the solution is more than 8. Under this pH, other kinds of yttrium vanadates are precipitated such as YV_3O_9 or $Y_2V_{10}O_{28}$.

Starting from this work, we studied the direct precipitation of yttrium orthovanadate from Y^{3+} and VO_4^{3-} salts in water. It was found that the pH of the vanadate solution must not be too high because this leads to the rapid precipitation of $Y(OH)_3$, which further reacts only very slowly with the vanadate ions. Optimization of the experimental conditions at room temperature led us to choose the following experimental conditions: 10 mL of a 0.1 mol L^{-1} solution of orthovanadate (Na_3VO_4) were first prepared by dissolving 1 equiv of metavanadate ($NaVO_3$) in an aqueous solution containing 3 equiv of NaOH. The initial pH of the solution was 13.5, which ensures a complete transformation of the metavanadate into the orthovanadate.[15] A 10 mL aliquot of a 0.1 mol L^{-1} aqueous solution of $Y(NO_3)_3$ and $Eu(NO_3)_3$ was added dropwise with a peristaltic pump. A white precipitate was immediately observed, and the pH of the solution was stabilized at 11 after 30 min. As discussed before, the amount of NaOH present during the precipitation is of crucial importance. The addition of 3 equiv was found to be a good compromise since lower values gave yellow powders characteristic of the presence of polyvanadate species[11,16] and larger values led to the irreversible precipitation of $Y(OH)_3$.

Colloidal suspensions of YVO_4:Eu were obtained from the crude precipitate by dispersion of the aggregates using sonification (Branson Sonifier 450 W) and stabilization of the particles with 0.1 equiv of sodium hexametaphosphate, $(NaPO_3)_{12-13}{\cdot}Na_2O$. The obtained suspension was then dialyzed in pure water for 12 h, both to achieve purification and to improve its stability. Slightly opalescent YVO_4:Eu colloids were finally obtained with a typical concentration of 0.05 mol L^{-1}. These colloids were stable for several months in a large pH range ($4 < pH < 12$).

Colloidal particles can be recovered as a powder by destabilization using a small amount of $Mg(NO_3)_2$, centrifuging, and drying. X-ray diffraction (XRD) studies were then performed on these powders using a Philips X-Pert diffractometer at Cu Kα radiation ($\lambda = 1.54$ Å). High-resolution transmission electron microscopy (HRTEM) was carried out on a on an AKASHI TOPCON 002B microscope operating at 160 kV (point resolution 1.8 Å, Cs = 0.4 nm). The samples for HRTEM were prepared by depositing a drop of colloidal solution on a carbon grid. Optical characterizations were conducted on diluted solutions (yttrium vanadate concentration around 5×10^{-4} mol L^{-1}). Dynamic light scattering experiments were carried out with a PCS light scattering equipment supplied by Malvern. Absorption spectra were recorded on a Shimadzu 1600 A spectrophotometer. Luminescence spectra as well as lifetime measurements were recorded on a Hitachi F-4500 spectrofluorometer. The quantum yields were determined by comparing the integrated emission of the colloidal solutions with the emission from a Rhodamine 6G solution in ethanol having the same optical density and excited at the same wavelength (280 nm).

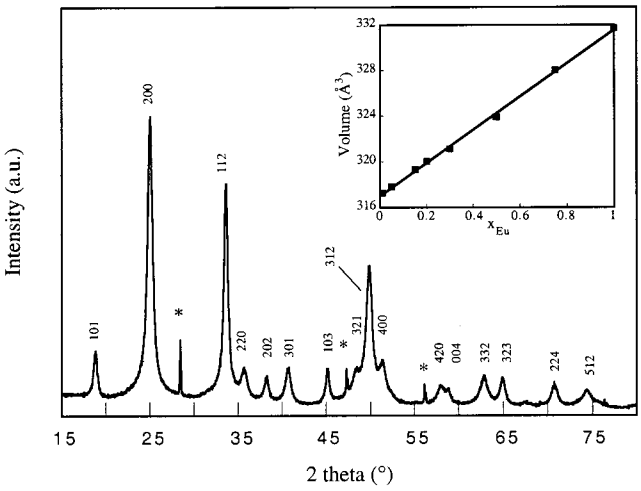

Figure 1. X-ray diffraction pattern (Cu Kα) performed on a powder of $Y_{0.95}Eu_{0.05}VO_4$ nanoparticles (peaks marked with a star correspond to the silicon reference). The inset shows the linear evolution of the unit cell volume (the *a* and *c* tetragonal parameters are refined from diffraction data) versus the europium fraction for the $Y_{1-x}Eu_xVO_4$ nanoparticles.

Results and Discussion

Structural Characterization of the Particles. The crystalline phases and coherence lengths of our samples were determined by XRD. Figure 1 shows a representative diagram in the case of the $Y_{0.95}Eu_{0.05}VO_4$ nanoparticle powder. This pattern is in agreement with the usual zircon-type structure of $EuVO_4$ or YVO_4.[17] Besides, XRD pattern of a powder treated at 1000 °C for 12 h does not show any peak corresponding to the Y_2O_3 phase. This confirms that our experimental conditions are well optimized for the almost exclusive precipitation of YVO_4 instead of $Y(OH)_3$.

XRD was also used to attest to the efficient and homogeneous incorporation of the Eu^{3+} ions as substituents for the Y^{3+} ions inside the YVO_4 host matrix. The method consists of plotting the volume of the tetragonal cell of a set of (Y, Eu)VO_4 samples as a function of *x*, the initial molar fraction of Eu^{3+} used for their aqueous preparation. The cell volume is determined by refining the tetragonal cell parameters from the diffraction data of each sample. As expected by the Vegard's law, the evolution of the volume of the unit cell is linear with *x* (inset Figure 1). This clearly demonstrates that the incorporation of Eu^{3+} in the YVO_4 matrix is quantitative for the nanoparticles, showing the $Y_{1-x}Eu_xVO_4$ single phase, where *x* equals to the initial fraction of Eu^{3+} used in the synthesis. Note that this result is not very surprising considering the similar chemical reactivities of the Eu^{3+} and Y^{3+} ions.

The size of the crystalline domains, as obtained from the width of the diffraction peaks using the Scherrer's law, is about 14 nm. This value is nevertheless averaged using all the distances deduced from the width of the different peaks. A systematic deviation is indeed clearly

(11) Arbit, E. A.; Serebrennikov, V. V. *Russ. J. Inorg. Chem.* **1965**, *10* (2), 220.
(12) Popov, V. I.; Bagdasarov, K. H. S.; Buseva, I. N.; Mokhosoev, M. V. *Sov. Phys. Crystallogr.* **1969**, *13*, 974.
(13) Touboul, M.; Popot, A. *Rev. Chim. Minér.* **1985**, *22*, 610.
(14) Ropp, R. C.; Carroll, B. *J. Inorg. Nucl. Chem.* **1977**, *39*, 1303–1307.
(15) Baes, C. F. Jr.; Mesmer, R. E. *The Hydrolysis of Cations*; Krieger Publishing Company; Malabar, FL, 1986.
(16) Erdei, S. *J. Mater. Sci.* **1995**, *30* (19), 4950.
(17) Schwarz. *Z. Anorg. Allg. Chem.* **1963**, *322*, 143.

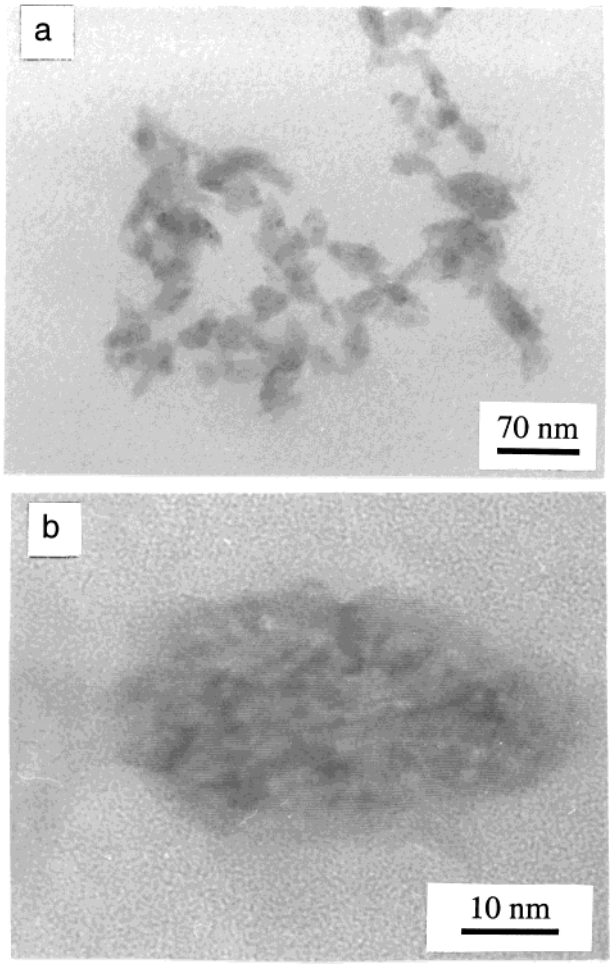

Figure 2. (a) TEM micrographs of $Y_{0.85}Eu_{0.15}VO_4$ crystalline nanoparticles. (b) Single particle photograph showing the ellipsoidal form.

observed, which tends to show some kind of anisotropy in the coherence length of the particles. Indeed, an ellipsoidal form of the particles was observed on the TEM photograph of a $Y_{0.85}Eu_{0.15}VO_4$ colloid (Figure 2). Anisotropic particles with two characteristic dimensions of around 15 and 30 nm can be clearly observed. Besides, the contrast observed within each particle suggests that they are polycrystalline, with numerous defects. This tends to show that the formation of the particles occurs through the aggregation of primary particles followed by a partial reorganization of the crystalline network.

The state of dispersion in the colloidal samples was deduced from dynamic light scattering experiments. Figure 3 shows a typical size distribution measured on a $Y_{0.85}Eu_{0.15}VO_4$ colloidal sample. The mean hydrodynamic diameter of the nanoparticles is about 40 nm with a standard deviation of 14 nm. This size distribution is in agreement with the one estimated from TEM observations, which indicates a good dispersion of the particles in the colloids.

Optical Properties of the Particles. The typical absorption spectrum of the YVO_4:Eu colloids is presented in Figure 4. The broad band, peaking at 272 nm, is attributed to a charge transfer from the oxygen ligands to the central vanadium atom inside the VO_4^{3-} ion. This band is almost the same as that observed in free VO_4^{3-} solutions, for which the maximum of absorption is 268 nm. Besides, Riwotzki and Haase[10] showed that the extinction coefficients for both species are nearly identical (4×10^3 dm^3 mol^{-1} cm^{-1}).

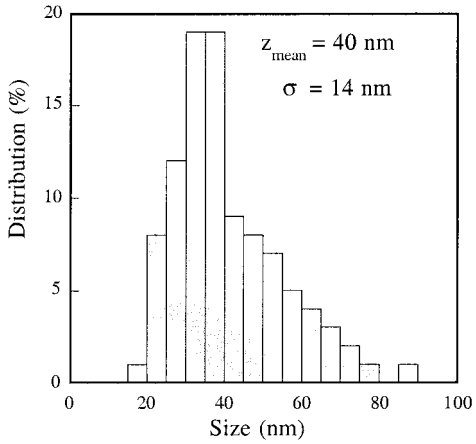

Figure 3. Size distribution for the $Y_{0.85}Eu_{0.15}VO_4$ colloidal sample deduced from dynamic light scattering experiments.

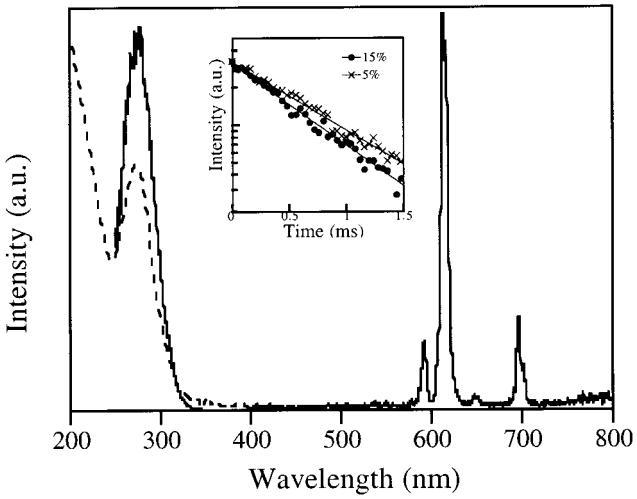

Figure 4. Absorption (dashed line), luminescence (λ_{ex} = 280 nm) and excitation spectra (λ_{em} = 615 nm) for the $Y_{1-x}Eu_xVO_4$ ($0 < x < 0.5$) colloids. The inset shows the $^5D_0$ lifetime decay curves for two samples (x = 0.05 and 0.15).

The luminescence spectrum (Figure 4) is very similar to the one observed in the case of YVO_4:Eu bulk samples. The intense emission at 615 nm is associated with the $^5D_0 - ^7F_2$ transition of the Eu^{3+} ion.[18] The corresponding excitation spectrum fits the absorption of the VO_4^{3-} species. This is in agreement with the mechanism known to be responsible for the luminescence in the bulk material. The absorption of UV photons by the VO_4^{3-} groups inside the host matrix is followed by a nonradiative transfer to the europium ions. These latter come back to the ground state through a radiative transition.

For the $Y_{1-x}Eu_xVO_4$ ($0 < x < 0.5$) colloids, the luminescence quantum yield presents a weakly marked maximum of 15% for an europium content around x = 0.3 (Figure 5a). Luminescence lifetimes of the europium $^5D_0$ level measured on the same set of samples are also presented in Figure 5b. By increasing x from 0 to 0.5, the lifetime continuously decreases from 1 to 0.4 ms.

(18) Brecher, C.; Samelson, H.; Lempicki, A.; Riley, R.; Peters, T. *Phys. Rev.* **1967** *155* (2), 178.

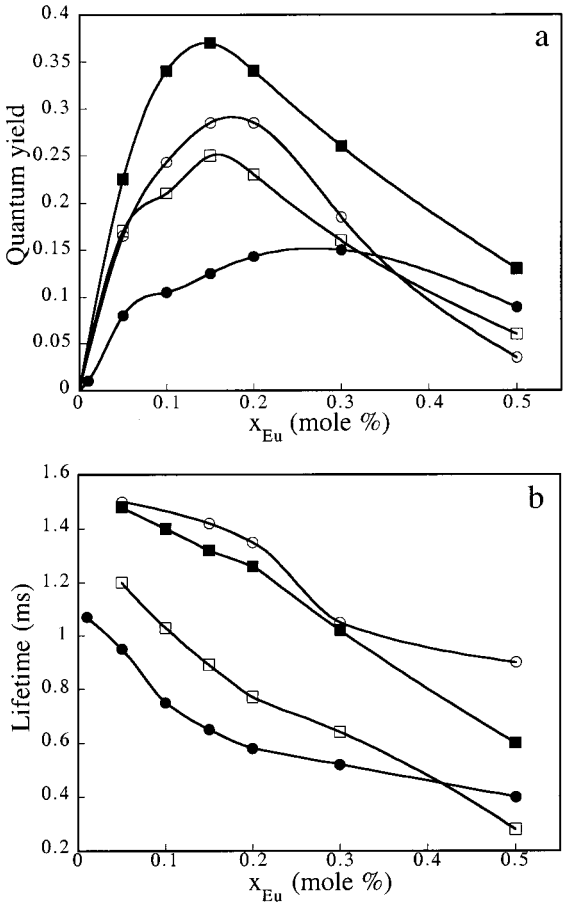

Figure 5. Luminescence quantum yields (a) and lifetimes of the europium $^5D_0$ level (b) for the $Y_{1-x}Eu_xVO_4$ ($0 < x < 0.5$) colloids: (●) as-prepared particles in water, (○) particles in D_2O, (□) particles in water after hydrothermal annealing, and (■) particles in D_2O after hydrothermal annealing.

This luminescence behavior contrasts with the one observed in the case of bulk materials, for which a quantum efficiency of 70% is found for an optimum europium content of 5% ($x = 0.05$),[19] with a corresponding luminescence lifetime of only 0.525 ms.[8]

Such differences obviously must be correlated to the microstructure of the nanoparticles. In addition to the limited coherence length of the nanocrystals, numerous bulk and surface defects exist as a consequence of the low-temperature synthesis and the high surface area of the crystallites. Some of these defects may act as nonradiative recombination centers and, therefore, may be responsible for the decrease of the quantum yield observed in the colloids.

In an attempt to characterize these nonradiative recombination centers, the surface has to be considered first since the size of the particles is on the same order of magnitude as the exciton diffusion length in the material.[20] As the particles are dispersed in water, their surface is covered by a large number of OH groups either chemically bonded to the surface or just adsorbed as water molecules. Such hydroxyl groups are well-known to be very efficient quenchers of the luminescence of lanthanide elements through multiphonon relaxation.[21] To quantify this surface effect, the colloids were transferred into deuterated water, which does not quench the luminescence of rare-earth elements. The effect of such a treatment can be seen in Figure 5, with the evolution of the luminescence quantum yield and lifetime of the europium $^5D_0$ level of the $Y_{1-x}Eu_xVO_4$ ($0 < x < 0.5$) colloids in deuterated water.

The observed increase of the quantum yield (up to 28%) as well as the lifetime of the $^5D_0$ level (up to 1.5 ms) demonstrates the importance of OH surface groups as multiphonon relaxation centers. Moreover, an optimum in the europium content is now clearly observed at about 16%. As in the bulk material, such an optimum is the result of the competition between the number of luminescent centers and the concentration quenching effect. This latter is due to the possible nonradiative transfer between closely located europium ions, which increases the mobility of the excited state within the host matrix. As a consequence, the probability of a nonradiative de-excitation via a luminescence killer is increased. In a material with numerous defects, the number of nonradiative pathways is high enough so that any increase of the mobility of the excited state will not significantly modify the probability for nonradiative de-excitations. As a consequence, since deuteration leads to a decrease of the nonradiative recombination centers, the concentration quenching becomes more effective and the optimum concentration more pronounced.

However, the luminescence behavior of the deuterated samples is still not as efficient as that in the bulk material. This may be the consequence of crystalline defects located within the particles. In fact, we have not observed any improvement when the complete synthesis of the particles is achieved in deuterated water, discrediting the presence of nonexchangeable hydroxyl groups inside the particles. To eliminate other defects inside the particles, hydrothermal treatments were carried out on colloids in water at 130 °C for 14 h. These conditions were found to change neither the coherence length nor the size of the particles. As shown in Figure 5, this thermal treatment clearly decreases the number of nonradiative recombination centers similarly to the previous deuteration treatment.

Finally, the hydrothermally treated colloids were transferred into the deuterated water. The important increase of the luminescence quantum yield shows that the deuteration and the thermal annealing are complementary treatments to decrease the number of nonradiative recombination centers. An interesting feature comes from the slight decrease of the lifetimes of the annealed and deuterated samples compared to those only deuterated. Knowing that the measured lifetime (τ) is connected to the radiative (τ_r) and nonradiative lifetimes (τ_{nr}) by the relation $1/\tau = 1/\tau_r + 1/\tau_{nr}$, such a behavior can only be interpreted by a decrease of the radiative lifetime of the europium $^5D_0$ level. A possible interpretation can be found in some distortions of the europium lattice site which lower the probability of a radiative transition. In this case, the influence of the thermal annealing can be understood as resulting from a relaxation of the lattice strains, leading to a decrease of the distortions. However, we note that the lifetimes of the annealed and deuterated samples are still higher than those in the bulk material. This suggests that, due

(19) Ropp, R. C. *J. Electrochem. Soc. Solid State Sci.* **1968**, *115* (9), 940.

(20) Hsu, C.; Powell, R. C. *J. Lumin.* **1975**, *10*, 273−293.

(21) Blasse, G. *Prog. Solid State Chem.* **1988**, *18*, 119.

to the conditions of synthesis, there are defects and distortions within the particles which cannot be easily eliminated.

Conclusion

We have presented a very simple and efficient chemical route to prepare highly luminescent colloids with a controlled composition in the $Y_{1-x}Eu_xVO_4$ ($0 < x < 1$) solid solution. These nanoparticles can easily be assembled as thin films by dip- or spin-coating techniques, allowing for the testing of them in the future as luminescent materials in different displays.

The nanocrystallites could also probably be useful as ultrasensitive biological labels because they are water-soluble and biocompatible. Moreover, in comparison with organic dyes and semiconductor quantum dots, they are narrower in spectral line width and probably more stable against photobleaching. However, further studies are required to improve the size control and the crystallinity and to study the possible grafting of molecular and biological species at the surface of particles.

Acknowledgment. We thank Y. Champion from the Centre d′Étude de Chimie Métallurgique in Vitry (France) for the HRTEM observations.

CM990722T